

Highly accurate fabric piezoresistive sensor with anti-interference of both high humidity and sweat based on hydrophobic non-fluoride titanium dioxide nanoparticle

Liyan Yang[#], Jun Ma[#], Weibing Zhong, Qiongzen Liu, Mufang Li, Wen Wang, Yi Wu,
Yuedan Wang, Xue Liu, Dong Wang^{*}

Hubei Key Laboratory of Advanced Textile Materials & Application, Hubei International Scientific and Technological Cooperation Base of Intelligent Textile Materials & Application, Wuhan Textile University, Wuhan, 430200, China

* Corresponding author: Dr. Liyan Yang and Dr. Prof. Dong Wang

E-mail: lyyang@wtu.edu.cn, wangdon08@126.com

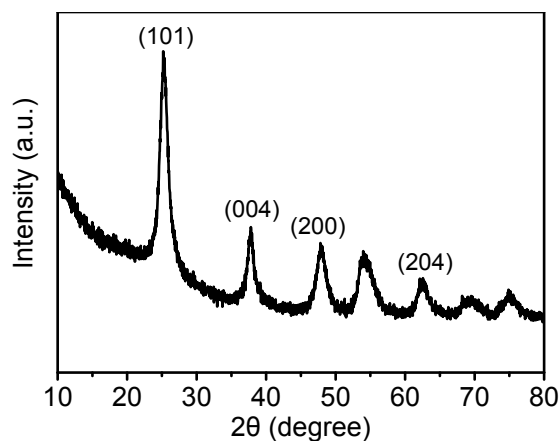


Fig. S1 XRD spectrum of the TiO₂ nanoparticle powders.

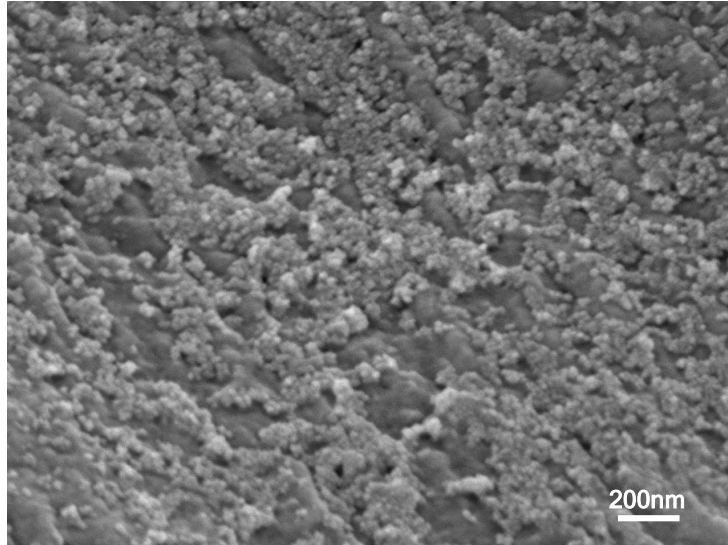


Fig. S2 The SEM images of TiO₂-ODI layer (local magnification of the insert in Fig. 1c).

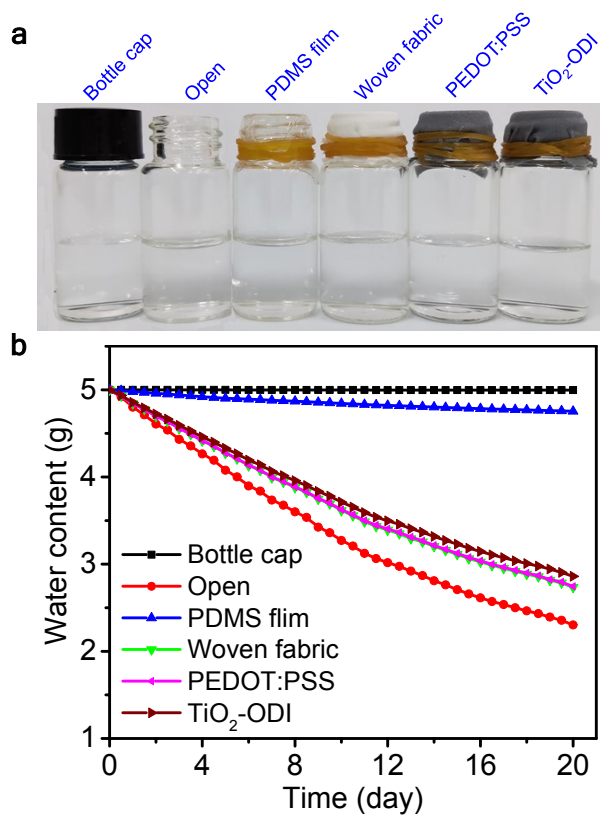


Fig. S3 Water vapor transmission tests. (a) Photograph of bottles covered by different substrates. The mass of the containing water in each bottle is 5.0 g. (b) The mass loss of the containing water was measured at ambient air (temperature of 25~30 °C, RH of 40~80 %).

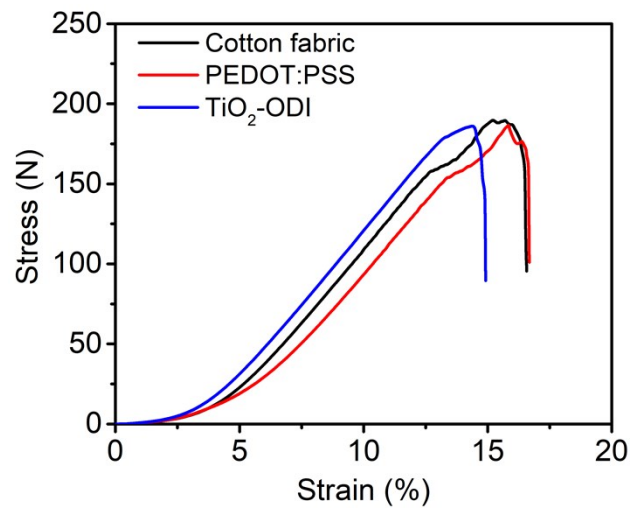


Fig. S4 The mechanical property of the cotton fabric, PEDOT:PSS pressure sensor, and TiO₂-ODI pressure sensor.

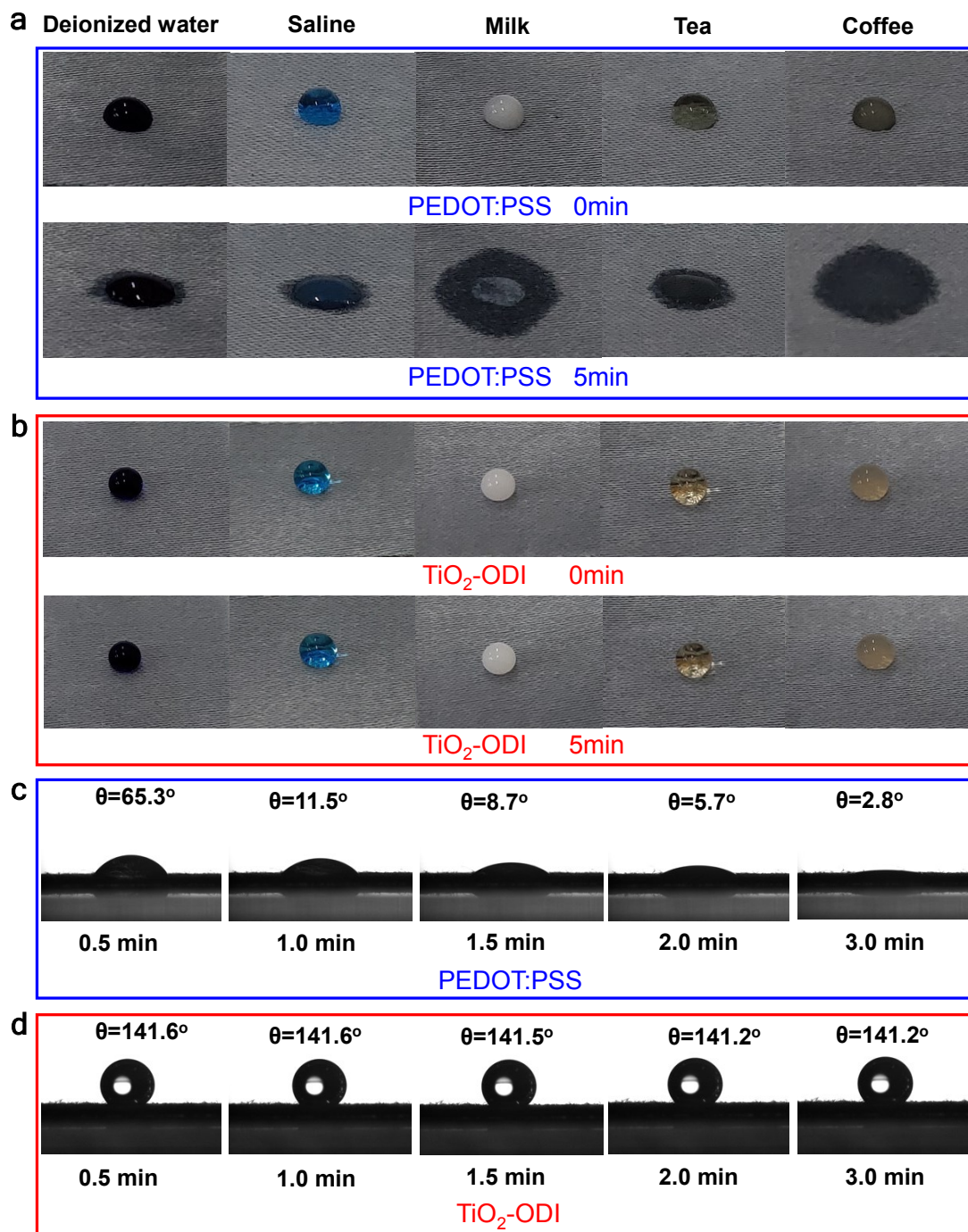


Fig. S5 The photographs of (a) PEDOT:PSS and (b) TiO₂-ODI layer dripped with deionized water, saline, milk, tea, and coffee for 0 and 5 mins, respectively. The volumes of the droplets are 5 μ L. The dynamic water contact angle of (c) PEDOT:PSS and (d) TiO₂-ODI layer from 0.5 to 3 mins.

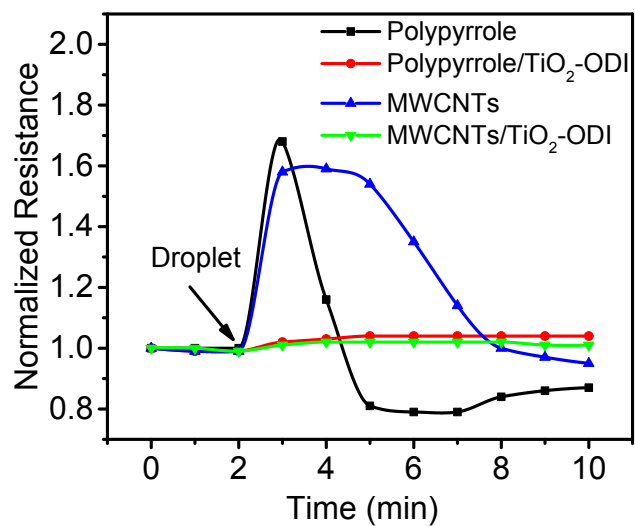


Fig. S6 The normalized resistance changes of the polypyrrole, polypyrrole/TiO₂-ODI, MWCNTs, and MWCNTs/TiO₂-ODI pressure sensors under saline droplets.

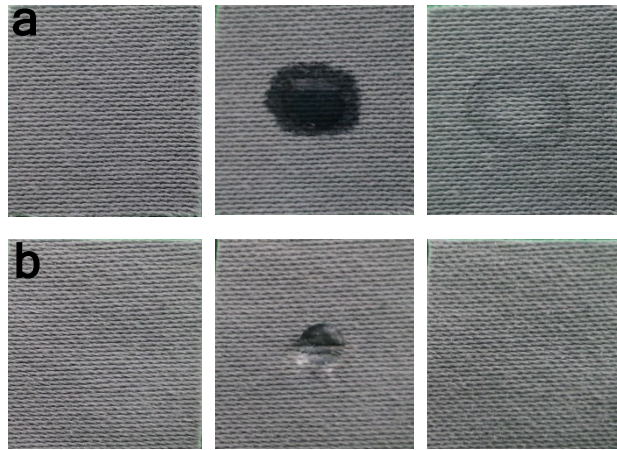


Fig. S7 The protective effect of the TiO₂-ODI layer. (a) PEDOT:PSS (up) and (b) TiO₂-ODI (down) samples were dripped with water and then dried in ambient air, respectively.

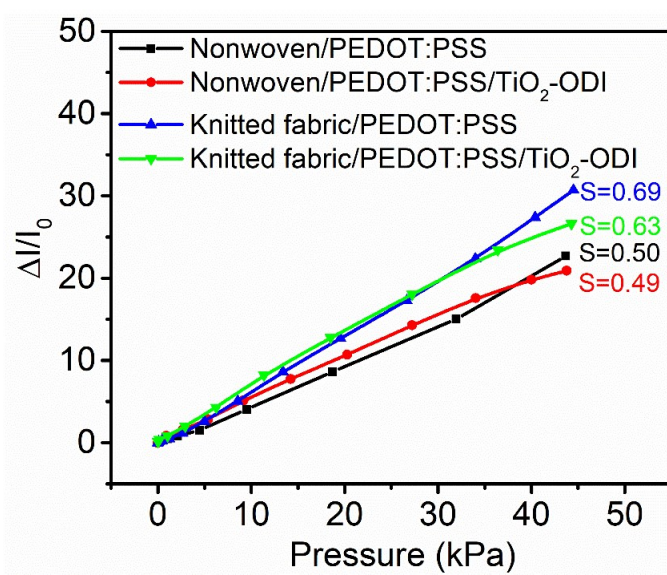


Fig. S8 The sensitivity of PEDOT:PSS pressure sensor and TiO₂-ODI pressure sensor based on the nonwoven and knitted fabric substrate.

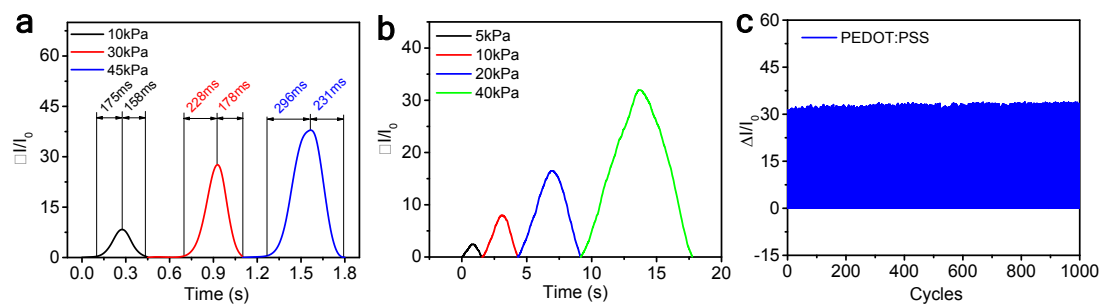


Fig. S9 (a) The response time of the PEDOT:PSS pressure sensor at different pressures. (b) The relative current change of the PEDOT:PSS pressure sensor under increased pressure from 5 kPa to 40 kPa. (c) The cycling stability test of the PEDOT:PSS pressure sensor during 1000 cycles.

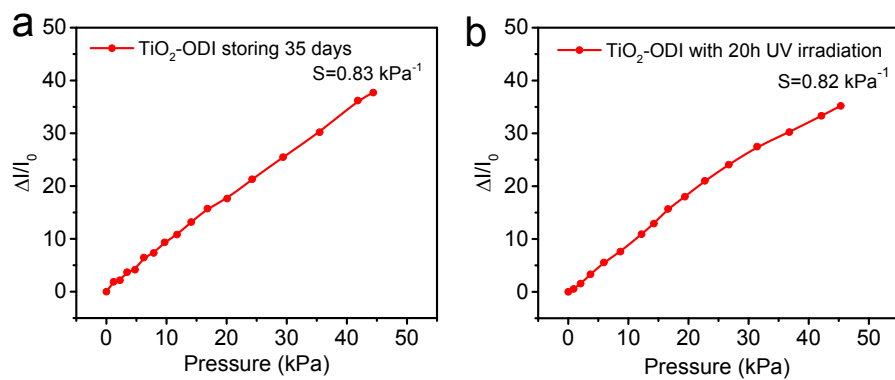


Fig. S10 The sensitivity of $\text{TiO}_2\text{-ODI}$ sensor (a) after storing in the sample cabinet for 35 days and (b) with 20h UV irradiation.

Table S1 The overall performance of the pressure sensors based on different hydrophobic materials

Hydrophobic materials	Substrate	Anti-interference of droplets	Anti-interference of high humidity	Permeability	Ultraviolet protection	Self-cleaning	Sensitivity (working range)	Reference
1H,1H,2H,2H-perfluorooctyltriethoxysilane (FAS) modified reduced graphene oxide	CNTs/chitosan aerogel	Water	-	Good	-	-	4.97 kPa ⁻¹ (0-3kPa)	1
PDMS film	Polyimide film	Water	-	Poor	-	-	0.05 kPa ⁻¹ (40-80kPa)	2
PET film	PET film	Water	-	Poor	-	-	6.4 kPa ⁻¹ (0-800kPa)	3
Perfluorodecyltriethoxysilane	PET Nonwoven	Water and sweat	-	Good	-	-	7.0 kPa ⁻¹ (0-25kPa)	4
rGO/SWCNTs	Cotton fabric	Water	-	Good	-	-	147.4 kPa ⁻¹ (0-50 kPa)	5
non-fluoride TiO ₂ -ODI nanoparticle	Cotton fabric	Water and sweat	Yes	Good	Yes	Yes	0.012 kPa ⁻¹ (1.27-12.7kPa)	Our work
							0.83 kPa ⁻¹ (0-48kPa)	

References

- 1 J. Wu, H. Li, X. Lai, Z. Chen and X. Zeng, *Chem. Eng. J.*, 2020, **386**, 123998.
- 2 Z. Gao, K. Jiang, Z. Lou, W. Han and G. Shen, *J. Mater. Chem. C*, 2019, **7**, 9648-9654.
- 3 H. Xu, L. Gao, Y. Wang, K. Cao, X. Hu, L. Wang, M. Mu, M. Liu, H. Zhang, W. Wang and Y Lu, *Nano-Micro Letters*, 2020, **12**, 159.
- 4 L. Zhang, J. He, Y. Liao, X. Zeng, N. Qiu, Y. Liang, P. Xiao and T. Chen, *J. Mater. Chem. A*, 2019, **7**, 26631-26640.
- 5 S. J. Kim, W. Song, Y. Yi, B. K. Min, S. Mondal, K. S. An and C. G. Choi, *ACS Appl. Mater. Inter.*, 2018, **10**, 3921-3928.